[7]M. M. Minor, SAM: Code for the Fixing of Experimental Parameters.
[8]F. G. Perey, Phys. Rev. 132, 755 (1963).
[9]C. M. Lederer, J. M. Hollander, and I. Perlman, *Table of Isotopes* (Wiley, New York, 1967), 6th ed.
[10]M. Goldhaber and R. D. Hill, Rev. Mod. Phys. 24, 179 (1952).
[11]I. Rezanka, J. Frana, A. Mastalka, and J. Benes, Nucl. Sci. Abstr. 31078 (1962).
[12]B. Harmatz, T. H. Handley, and J. W. Mihelich, Phys. Rev. 119, 1345 (1960).
[13]H. Verheul, H. M. W. Booy, J. G. R. Okel, and J. Blok, Nucl. Phys. 42, 551 (1963).
[14]F. M. Bernthal, Ph.D. thesis, University of California at Berkeley, 1969 (unpublished).
[15]F. M. Bernthal, J. O. Rasmussen, and J. M. Hollander, Phys. Rev. C 3, 1294 (1971).
[16]K. Brandi, R. Engelmann, V. Hepp, E. Kluge, H. Krehbiel, and V. Meyer-Berkhout, Nucl. Phys. 59, 33 (1964).
[17]J. Borggreen, N. J. H. Hansen, J. Pedersen, L. Westgaard, J. Zylicz, and S. Bjornholm, Nucl. Phys. A96, 561 (1967).
[18]K. Neergard and P. Vogel, Nucl. Phys. A145, 33 (1970).
[19]M. M. Minor, E. Jurney, and R. K. Sheline, private communication.
[20]O. Mikoshiba, R. K. Sheline, and T. Udagawa, Nucl. Phys. A101, 202 (1967).
[21]A. Namenson, H. E. Jackson, and R. K. Smither, Phys. Rev. 146, 844 (1966).
[22]L. Varnell, J. H. Hamilton, and R. L. Robinson, Bull. Am. Phys. Soc. 16, 1156 (1971).
[23]J. Kern, O. Mikoshiba, R. K. Sheline, T. Udagawa, and S. Yoshida, Nucl. Phys. A104, 642 (1967).

PHYSICAL REVIEW C VOLUME 6, NUMBER 2 AUGUST 1972

^{142}Ce(d,p) and ^{142}Ce(d,t) Reactions and Isobaric Analog Resonances in ^{142}Ce(p,p_0) and ^{142}Ce(p,p_1)†

L. Lessard, S. Gales,* and J. L. Foster, Jr.
Laboratoire de Physique Nucléaire, Département de Physique, Université de Montréal, Montréal, Québec, Canada
(Received 10 March 1972)

The reactions ^{142}Ce(d,p) and ^{142}Ce(d,t) at an incident deuteron energy of 12.6 MeV have been investigated with an energy resolution of about 16 keV, and excitation functions for the reactions ^{142}Ce(p,p_0) and ^{142}Ce(p,p_1) have been measured from 9.5- to 12-MeV incident proton energies. The analysis of the analog resonances observed in the excitation functions is compared with the results of the ^{142}Ce(d,p) experiment.

I. INTRODUCTION

The shell-model structure of the 82-neutron nuclei is now rather well known from pickup and stripping reactions[1-3] and from the decay of isobaric analog resonances.[4-6] The modification of this structure as one goes away from the closed 82-neutron shell is also of interest. As part of an over-all study of (82+2)- and (82+3)-neutron nuclei we have investigated the reactions ^{142}Ce(d,p) and ^{142}Ce(d,t) and the analog resonances in the reactions ^{142}Ce(p,p_0) and ^{142}Ce(p,p_1).

The elastic scattering experiment supplements and serves as a comparison to the (d,p) results. In the analysis of the reaction ^{141}Ce(p,p_1), results from the other three experiments are directly employed in an attempt to measure coupling of single neutron orbitals to the 2_1^+ level of ^{142}Ce in the wave functions of several states in ^{143}Ce.

The previous ^{142}Ce(d,p) and ^{142}Ce(d,t) measurements by Fulmer, McCarthy, and Cohen[7] were made with natural cerium, 11% ^{142}Ce, and a resolution of about 50 keV. The analog of the first excited state of ^{143}Ce has been observed by Graw *et al.*[8]

II. EXPERIMENTAL PROCEDURE

Proton and deuteron beams of the Université de Montréal Model EN tandem Van de Graaff accelerator were incident upon isotopically separated 92.7% ^{142}Ce and 7.3% ^{140}Ce targets. The excitation functions ^{142}Ce(p,p_0) and ^{142}Ce(p,p_1) were taken at proton laboratory energies from 9.6 to 12.0 MeV in steps of typically 10 keV. The scattered particles were detected by an array of four surface-barrier detectors cooled to −15°C at laboratory angles of 170, 160, 150, and 140°. The four counters were routed into two analog-to-digital converters (ADC) with direct access to the memory of an on-line CDC 3100 computer.

A 12.6-MeV incident deuteron beam, collimated

to a diameter of $\frac{1}{16}$ in. was used for the ^{142}Ce(d, p) and ^{142}Ce(d, t) experiments. The reaction products were detected by two cooled 2000-μm-depletion-depth surface-barrier detectors mounted 10° apart on the scattering chamber turntable. The detector collimators subtended about 2° in the scattering plane. The energy resolutions were 15.5 and 17.5 keV for the two detectors. To minimize ADC dead time, the regions above and below the deuteron elastic peak were treated separately by the analyzers and stored in separate 2048 memory regions. Figure 1 shows a sample spectrum for the region above the deuteron elastic peak. This region contains 56 proton groups from the ^{142}Ce(d, p) reaction. Other weak proton groups were seen at higher excitation energy but they have not been analyzed because of high background and the presence of contaminant elastic peaks. Energies were determined by using the known energy differences of the observed proton groups from ^{140}Ce(d, p) and ^{16}O(d, p). They are believed to be accurate to ±5 keV for the stronger states and ±10 keV for the weaker ones. Angular distributions were obtained for 30 states at angles from 15 to 90°. Figure 2 shows a portion of a spectrum below the deuteron elastic peak which contains five triton peaks from the ^{142}Ce(d, t) reaction. The measured ground-state Q values for the ^{142}Ce(d, p) and ^{142}Ce(d, t) reactions are shown in Table I and compared with the previously determined values.[9, 10]

For both sets of experiments absolute cross sections were measured in the same fashion. The product of the solid angle subtended by a given detector and the target thickness was determined at 4.0 MeV, assuming that at that energy the elastic scattering of protons and deuterons by ^{142}Ce is purely Rutherford scattering. The same target angle was then kept throughout the experiments. The absolute cross sections in this work are estimated to be accurate to ±10%, independent of statistics.

Target preparation presented special problems. A tungsten crucible, containing a mixture of CeO and thorium, was heated through electron bombardment. Reduction of the ceric oxide to metallic cerium by the thorium and evaporation of the cerium occurred simultaneously. Targets were typically 50 μg/cm^2 Ce on 20-μg/cm^2 carbon foils with a thorium contamination of about 10%.

The accelerator energy calibration is believed to be accurate to within 20 keV at 10 MeV.

III. ANALYSIS

A. Optical Model

In order to verify optical-potential parameters for the distorted-wave Born-approximation (DWBA) analysis of the (d, p) and (d, t) experiments and for the determination of single-particle widths for the analog resonances, deuteron and proton

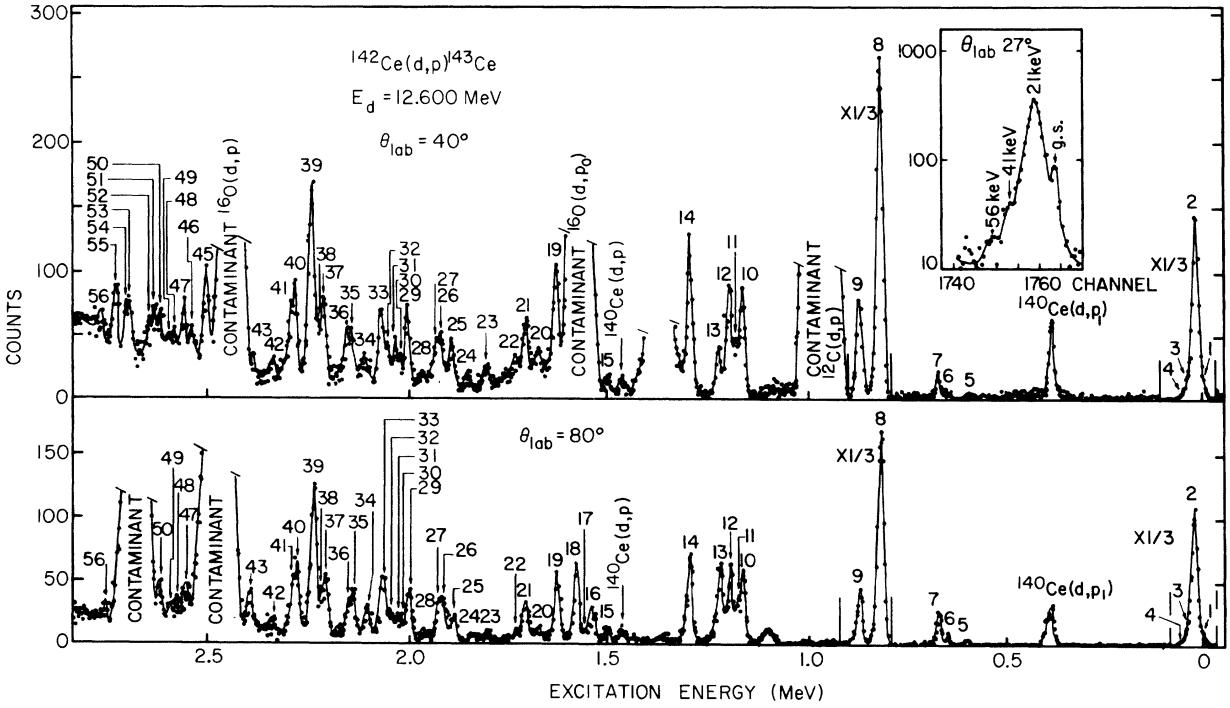

FIG. 1. Spectra from ^{142}Ce(d,p). The square in the upper right corner shows the ground-state multiplet in detail at 27°.

elastic angular distributions were taken at 12.6 and 12.0 MeV, respectively. At this proton energy the effect of the analog resonances should be negligible.

Table II shows the deuteron and proton optical-model parameters obtained by fitting the experimental data with code MAGALI.[11] The starting values of the parameters were chosen from the average values of Perey.[12, 13] In the fitting procedure the geometry parameters (and the spin-orbit potential for the proton) were kept fixed and only the real and imaginary potential depths allowed to vary. Two different proton potentials giving comparable fits were obtained. Proton potential A of Table II was used in the DWBA calculations because it gave considerably better fits to the (d, p) angular distributions. Figure 3 shows the deuteron and proton (potential A) elastic optical-model fits.

At forward angles the thorium and Ce elastic peaks were not separated and the estimated contribution of the thorium was subtracted. The surface of the thorium peak was determined from a standard optical model which fitted the backward-angle data. The error in this procedure should be very small as the deviation of the optical-model calculation from Rutherford scattering was only a few percent.

TABLE I. Measured ground-state Q values (in MeV) of the ^{142}Ce(d, p) and ^{142}Ce(d, t) reactions.

Reaction	This work	Mass table (Ref. 9)	Ref. 10
^{142}Ce(d, p)^{143}Ce	2.945 ± 0.015	2.880 ± 0.050	2.960
^{142}Ce(d, t)^{141}Ce	−0.909 ± 0.015	−0.953 ± 0.050	

For the tritons the average potential of Becchetti, Jr., and Greenlees,[14] was employed.

B. Distorted-Wave Analysis

The DWBA calculations for the analysis of the data were performed using computer code DWUCK.[15] Spectroscopic factors S were computed by comparing DWBA predictions with the measured cross-section values,

$$\left(\frac{d\sigma}{d\Omega}\right)_{\text{exp}} = SN\left(\frac{d\sigma}{d\Omega}\right)_{\text{DWBA}}.$$

Assuming a spin-zero target, $N = 1.53(2J_f + 1)$ for a (d, p) reaction[15, 16] and $N = 3.33$ for the (d, t) case,[15, 17] where J_f is the final-state spin. Figures 4–6 show, respectively, families of $l = 1$, 3, and 5.

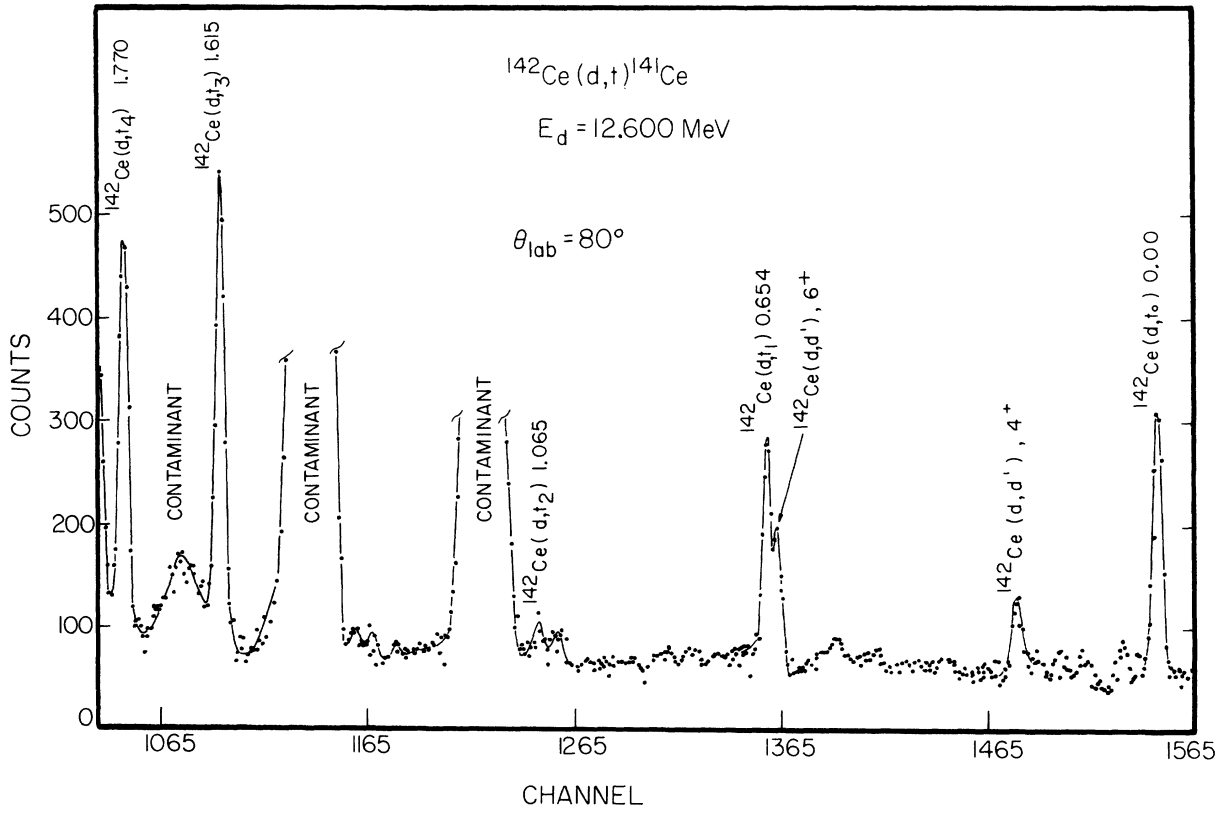

FIG. 2. Spectrum from ^{142}Ce(d, t).

TABLE II. Optical-model parameters used in the ^{142}Ce(d,p) and ^{142}Ce(d,t) distorted-wave calculations: The optical potential is

$$U(r) = V_C - V_0 f(r, r_0 A^{1/3}, a) - i W_V f(r, r_i A^{1/3}, a_i) + 4i W_D a_i \frac{d}{dr} f(r, r_i A^{1/3}, a_i) + \vec{\sigma}\cdot\vec{l} \left(\frac{\hbar^2}{m_\pi c}\right)^2 \frac{V_{so}}{r} \frac{d}{dr} f(r, r_{so} A^{1/3}, a_{so}),$$

where

$f(r, r_0 A^{1/3}, a) = \{1 + \exp[(r - r_0 A^{1/3})/a]\}^{-1}$ is the usual Woods-Saxon shape.

	Real-well parameters							Imaginary-well parameters			
Channel	V_0 (MeV)	a (fm)	r_C (fm)	r_0 (fm)	V_{so} (MeV)	a_{so} (fm)	r_{so} (fm)	W_V (MeV)	W_D (MeV)	a_i (fm)	r_i (fm)
Proton A	53.8	0.65	1.25	1.25	6.25	0.65	1.25		10.7	0.65	1.25
Proton B	55.5	0.65	1.25	1.25	6.25	0.65	1.25		18.1	0.47	1.25
Deuteron	100.8	0.81	1.25	1.15					16.2	0.68	1.34
Triton	162.0	0.72	1.25	1.20	2.5	0.72	1.20	23.0	0.00	0.84	1.40

Finite range (when included): $R_{dp} = 0.621$ $R_{dt} = 0.845$
Nonlocality (when included): $\beta_p = 0.85$ $\beta_d = 0.54$ $\beta_t = 0.20$
Form factor: $r_0 = 1.25$ $a = 0.65$ $V_{so} = 6.25$ $\beta_n = 0$
r_C = uniform charge radius

angular distributions with their DWBA predictions for the ^{142}Ce(d,p) reaction.

The distorted-wave calculations for the p- and f-wave states are in excellent agreement with the data, and variations in shape of the $l=1$ angular distributions with excitation energy are nicely

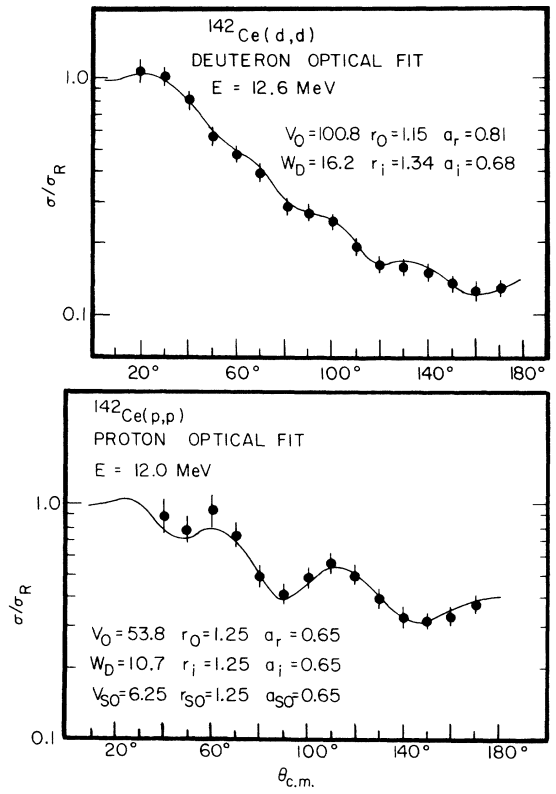

FIG. 3. Fits for optical potentials.

reproduced. Table III shows the spectroscopic factors, l values, and excitation energies for the observed levels. The spin identifications indicated will be discussed in Sec. IV. The DWBA calculations were made with nonlocality corrections to the deuteron and proton potentials and with a finite-range correction. No inner cutoff was used. A study of the influence of these corrections was made for the 0.020-MeV state. The corrections produce a decrease in S_{dp} of about 5% with no appreciable variation of the shape. Spectroscopic factors were determined from the best visual fit to the first maximum for the $l=3$ and $l=5$ angular distributions and from the region between the first and second maxima for those angular distributions characteristic of $l=1$. Proton potential A (see Table II) gave better fits to the observed angular distributions and was used for all results shown in this work. Spectroscopic factors calculated from Set A were from 5 to 10% larger than those calculated from Set B.

Figure 7 shows the ^{142}Ce(d,t) experimental data with DWBA predictions. Table IV shows $S/(2J+1)$ for the observed levels and a comparison with the results of Fulmer, McCarthy, and Cohen.[7] The subscript 1 refers to zero-range local-potential calculations. Subscript 2 refers to calculations with correction for finite range in the n-d interaction and for nonlocality in the optical potentials in entrance and exit channels employing options available in program DWUCK. The nonlocality ranges $\beta_d = 0.54$ and $\beta_t = 0.20$ are those used by Bassel[17] for the deuteron and ^{3}He. No inner cutoffs were used. The finite-range correction gave theoretical cross sections about 30% greater than

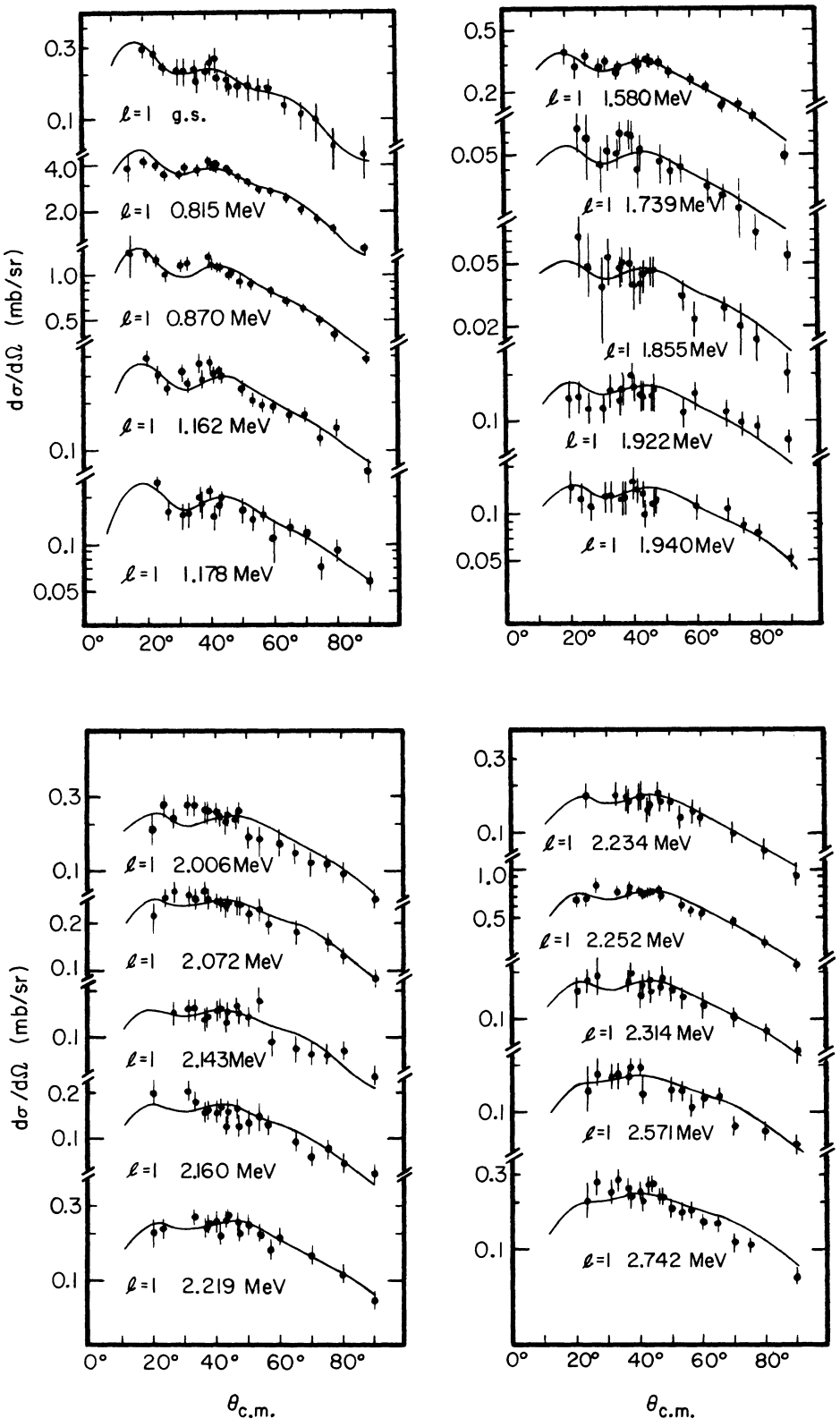

FIG. 4. Angular distributions from ^{142}Ce(d,p) with $l = 1$ angular momentum transfer. The curves represent DWBA calculations for the spectroscopic factors shown in Table III.

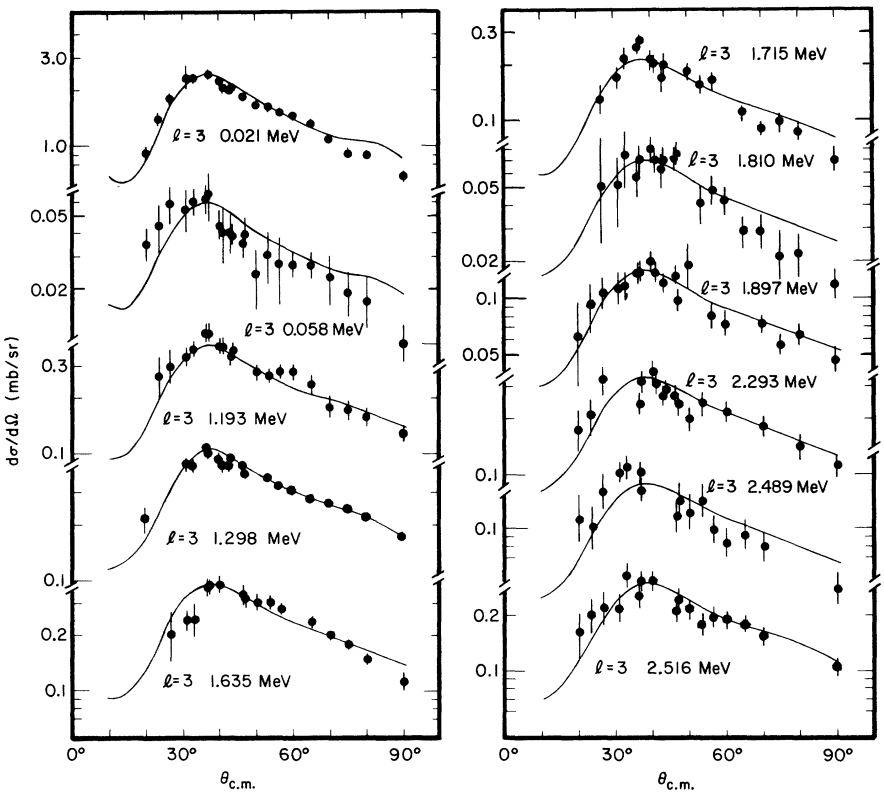

FIG. 5. Angular distributions from ^{142}Ce(d,p) with $l=3$ angular momentum transfer. The curves represent DWBA calculations for the spectroscopic factors shown in Table III.

the zero-range calculation with no significant changes in shape. The effect of the nonlocality corrections is negligible.

C. Elastic Scattering Resonance Analysis

Isobaric analog resonances in proton elastic scattering may be described as Breit-Wigner resonances plus nonresonant potential scattering.[18] For protons incident upon a zero-spin target, the differential cross section may be expressed[19] in terms of coherent and incoherent scattering amplitudes A and B as

$$\frac{d\sigma}{d\Omega} = |A|^2 + |B|^2 .$$

By assuming that for the nonresonant scattering the spin-flip contribution is negligible, it is possible to express the amplitudes A and B as

$$A = \rho e^{i\gamma} + \frac{1}{2k}\sum_{l,J}(J+\tfrac{1}{2})\frac{e^{i\alpha_{lJ}}\Gamma_{p_0}^{lJ}}{(E_J-E)-\frac{1}{2}i\Gamma_T}P_l^0(\cos\theta),$$

$$B = -\frac{1}{2k}\sum_{l,J}(-1)^{l+J+1/2}\frac{ie^{i\alpha_{lJ}}\Gamma_{p_0}^{lJ}}{(E_J-E)-\frac{1}{2}i\Gamma_T}P_l^1(\cos\theta).$$

Here $\alpha_{lJ}=2\omega_l+2\varphi_l+\zeta_l-\gamma$, where φ_l is the resonance mixing phase, ω_l is a relative Coulomb phase, and ζ_l is the real part of the optical phase, $\delta_l=\zeta_l+i\xi_l$. The optical phases are assumed to be independent of J. The nonresonant background

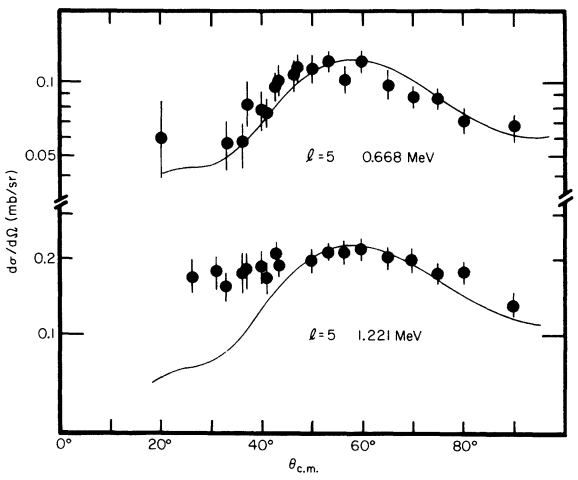

FIG. 6. Angular distributions from ^{142}Ce(d,p) with $l=5$ angular momentum transfer. The curves represent DWBA calculations for the spectroscopic factors shown in Table III.

amplitude is given by the quantity

$$\rho e^{i\gamma} = -\frac{\eta}{2k}\csc^2(\tfrac{1}{2}\theta)\exp\{-i\eta\ln[\sin^2(\tfrac{1}{2}\theta)]\}$$

$$+\frac{1}{2k}i\sum_{l,J}(2J+1)e^{2i\omega_l}[1-e^{2i\gamma_l}]P_l^0(\cos\theta),$$

where η is the Coulomb parameter, k the wave number, and ρ and γ are real.

These equations are incorporated into a computer code BRIGIT[20-22] in which ρ is represented as a fourth-degree polynomial in inverse powers of energy E:

$$\rho = A + B\frac{1}{E} + C\frac{1}{E^2} + D\frac{1}{E^3} + F\frac{1}{E^4} .$$

The program then searches for the best values of the background coefficients A, B, C, D, and F, and resonance parameters, E_J, Γ_T, $\Gamma_{p_0}^{lJ}$, and α_{lJ}.

Figures 8 and 9 show the ^{142}Ce(p, p_0) excitation functions and fits. For a given resonance, the first determination of the resonance parameters was made at the angle where the effect of the resonance was the most prominent. The parameters were then varied so as to give the best over-all

TABLE III. Summary of results from the reaction ^{142}Ce(d, p)^{143}Ce: energy levels and spectroscopic factors.

States	E_x (MeV)	L	J^π	S_{dp}	$(2J+1)S_{dp}$	States	E_x (MeV)	L	J^π	S_{dp}	$(2J+1)S_{dp}$
1	0.0	1	$\frac{3}{2}^-$		0.13	29	2.006	1			0.09
2	0.021	3	$\frac{7}{2}^-$	0.50	4.00	30	2.028				
3	0.040	(1)			0.08	31	2.040				
4	0.056	3	$(\frac{5}{2}^-)$		0.10	32	2.056				
5	0.598					33	2.072	1			0.12
6	0.637	(1)				34	2.112				
7	0.668	5	$\frac{9}{2}^-$	0.26	2.65	35	2.143	1			0.07
8	0.815	1	$\frac{3}{2}^-$	0.50	2.00	36	2.160	1			0.07
9	0.869	1	$(\frac{1}{2}^-)$	0.32	0.60	37	2.219	1			0.09
10	1.162	1			0.13	38	2.234	1			0.07
11	1.178	1			0.09	39	2.252	1	$(\frac{1}{2}^-)$	0.13	0.29
12	1.195	3	$(\frac{5}{2}^-)$	0.10	0.55	40	2.293	3			0.36
13	1.221	5	$\frac{9}{2}^-$	0.44	4.40	41	2.314	1			0.05
14	1.298	3	$(\frac{5}{2}^-)$	0.12	0.73	42	2.348				
15	1.506	3			0.13	43	2.413				
16	1.542					44	2.489	3			0.18
17	1.558	3			0.09	45	2.516	3			0.31
18	1.580	1			0.13	46	2.552				
19	1.635	3			0.47	47	2.571	1			0.07
20	1.680					48	2.596				
21	1.714	3			0.26	49	2.611				
22	1.739	1			0.02	50	2.630				
23	1.810	3			0.08	51	2.644				
24	1.855	1			0.02	52	2.660				
25	1.897	3			0.17	53	2.695				
26	1.922	1			0.07	54	2.712				
27	1.940	1			0.05	55	2.742	1			0.09
28	1.977					56	2.775				

fit at the four angles with a unique set of parameters for each resonance (i.e., the same energy, partial width, total width, and consistent phases). Because of the relatively large number of states in the region from 10.7 to 11.4 MeV the parameters for resonances in that region should be considered as only approximate. Although the most important feature of this region in the (d, p) work is a $\frac{9}{2}^-$ state it was impossible to see the effect of this state among its lower-spin neighbors. The target contained 7.3% ^{140}Ce and the resonances in the ^{140}Ce$+p$ system are clearly visible in our elastic excitation curves. To compensate for the effects of these resonances they were included in the fitting procedure with their parameters fixed at the values of Wurm, Heusler, and von Brentano.[23]

D. Analog State Spectroscopic Factors

Table V shows the resonance parameters and spectroscopic factors S_{pp} from the elastic excitation curve analysis. For a spin-zero target,

$$S_{pp} = (2T_0 + 1)\gamma_p^2/\gamma_{sp}^2,$$

where γ_{sp}^2 is the reduced width for a single-particle state, $T_0 = \frac{1}{2}(N - Z)$ is the target isospin, and γ_p^2 is the proton reduced width.

Thompson, Adams, and Robson[18] have devised a method to evaluate this expression. A bound-neutron wave function is used to determine γ_{sp}^2 by

$$\gamma_{sp}^2 = (\hbar^2/2ma_c)u_n^2(a_c),$$

where $u_n(r)$ is the radial neutron wave function for a single-particle state at the energy of the parent analog, $u_n^2(r)$ being normalized to unit integral over all space, m is the neutron mass, and a_c is the channel radius. The R-matrix theory is reformulated in terms of optical-model wave functions so that the boundary value matching can occur inside the nuclear interaction radius, thus taking into account that the charge-independence region is smaller than the region of nuclear interaction. The reduced partial width can be shown to be related to the "observed" partial width Γ_{p_0} by the relation

$$\Gamma_{p_0}^{lJ} = 2P_{lJ}^{\text{opt}}(a_c)e^{-2\xi_{lJ}}\gamma_p^2(a_c),$$

where P_{lJ}^{opt} is an optical-model penetrability,[18] and ξ_{lJ} is the imaginary part of the optical phase shift for angular momentum l and spin J. Similarly a single-particle width may be defined by

$$\Gamma_{sp}^{J} = \frac{1}{2T_0 + 1)} 2P_{lJ}^{\text{opt}}(a_c)e^{-2\xi_{lJ}}\gamma_{sp}^2(a_c).$$

Then

$$S_{pp} = \Gamma_{p_0}^{lJ}/\Gamma_{sp}^{J}.$$

A computer program ANSPEC[18] was used to evaluate these expressions and calculate spectroscopic factors.

By definition S_{pp}, although evaluated at a given value of the matching radius a_c, should be independent of the chosen value of a_c. In practice, such is not the case, since one assumes the nuclear forces to be charge independent in the interior region, which is obviously not true for any value of a_c. Outside the nucleus, the parent-state wave function must describe an outgoing wave. As a result, the calculated γ_p^2 value is larger than the correct value in the external region. On the other hand, for decreasing radii, one would expect γ_{sp}^2 to go to zero at the values of a_c for which the bound-neutron wave function vanishes. Near the nuclear surface the calculated S_{pp} is nearly constant over an interval of several Fermi with a flat minimum which was taken as the value of the spectroscopic factor.

The spectroscopic factors extracted from the ^{142}Ce(p, p_0) and ^{142}Ce(d, p) experiments are shown for comparison in Table V. The agreement between the values obtained for the eight states for

TABLE IV. Summary of results from ^{142}Ce(d, t). The S_{dp}^* are spectroscopic factors (Ref. 3) from the reaction ^{140}Ce(d, p); S_1/S_{dp}^* is calculated as an estimate of the total occupation of the subshell J^π in the ground state of ^{142}Ce. $V_J^2 = (S_1/S_{dp}^*)/(2J + 1)$.

E (MeV)	l	J^π	$\frac{S_1}{2J+1}$	$\frac{S_2}{2J+1}$	S_{dp}^*	$\frac{S_1}{S_{dp}^*}$	V_J^2
0.00	3	$\frac{7}{2}^-$	0.15	0.11	0.9	1.3	0.16
0.655	1	$\frac{3}{2}^-$	0.08	0.06	0.5	0.7	0.17
1.065	(1)	$(\frac{1}{2}^-)$	(<0.02)	(<0.02)	0.4	(<0.07)	0.03
1.615	2	$\frac{3}{2}^+$	0.68	0.51	...	...	
1.775	0	$\frac{1}{2}^+$	0.70	0.50	...	...	
2.140	(5)	$(\frac{11}{2}^-)$	(0.32)	(0.23)	...	...	

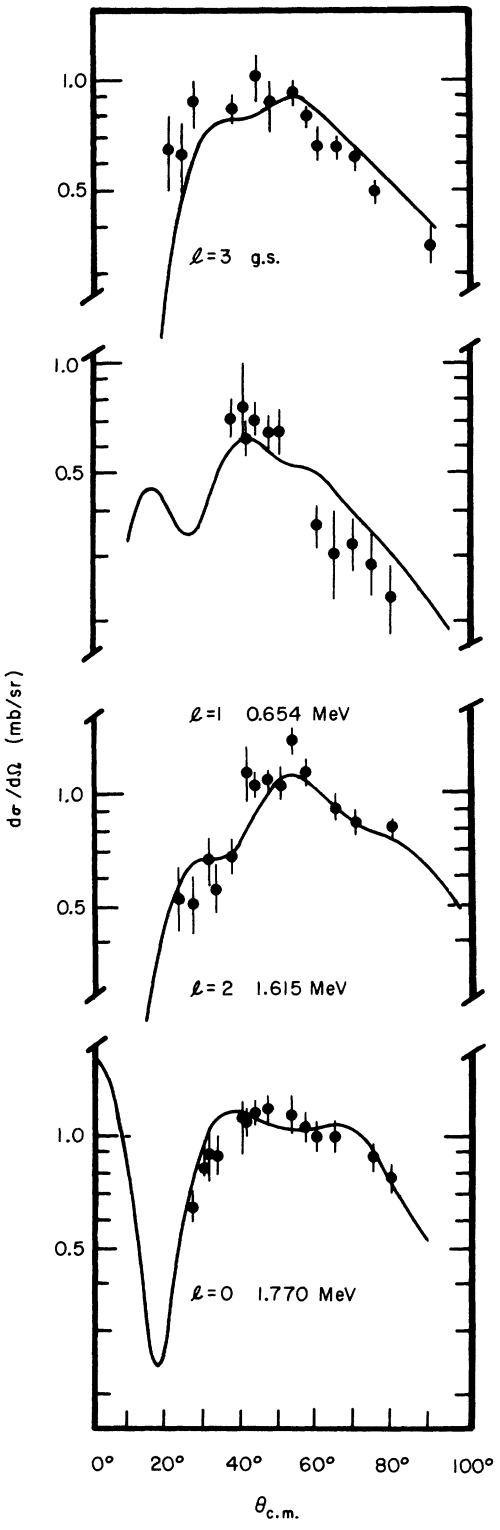

FIG. 7. Angular distributions from ^{142}Ce(d,t). The curves represent DWBA calculations for spectroscopic factors shown in Table IV.

which a comparison can be made is fairly good, even though the elastic values for the states at 1.162, 1.178, 1.195, 1.298, and 1.506 MeV can be considered as less reliable than the corresponding (d, p) results, because of the high density of states leading to overlapping resonances.

The same proton optical potential was used for the spectroscopic factor calculation by ANSPEC as for the DWBA analysis of the (d, p) experiment.

E. Inelastic Scattering Analysis

Figure 10 shows the ^{142}Ce(p, p_1) 2^+ excitation function at 170° compared with the elastic scattering excitation curve and the ^{142}Ce(d, p) spectrum. While in principle a detailed analysis is possible, overlapping levels and considerable interference between resonant and nonresonant scattering complicate the problem beyond the scope of this paper. Information can, however, be extracted from relatively crude considerations.

The wave function of a state in the ^{142}Ce$+n$ system (the "parent state") may be written[4] as

$$\Psi_J = \alpha(n_J \otimes \Phi_0) + \sum_{jk} \beta_{jk}(n_j \otimes \Phi_k^*)_J , \tag{1}$$

where Φ_0 represents the ground state and Φ_k^* the excited states of ^{142}Ce. The n_J and n_j refer to the essentially empty $2f_{7/2}$, $3p_{3/2}$, $1h_{9/2}$, $3p_{1/2}$, $2f_{5/2}$, and $1i_{13/2}$ subshells. The analog of this state is

$$\begin{aligned} T^-\Psi_J = {} & \frac{\alpha}{(2T_0+1)^{1/2}}(p_J \otimes \Phi_0) && \text{term I} \\ & + \frac{\alpha\sqrt{2T_0}}{(2T_0+1)^{1/2}}(n_J \otimes T^-\Phi_0) && \text{term II} \\ & + \sum_{jk} \frac{\beta_{jk}}{(2T_0+1)^{1/2}}(p_j \otimes \Phi_k^*)_J && \text{term III} \\ & + \sum_{jk} \frac{\beta_{jk}\sqrt{2T_0}}{(2T_0+1)^{1/2}}(n_j \otimes T^-\Phi_k^*)_J && \text{term IV}. \end{aligned} \tag{2}$$

Here $T^-\Phi_0 = (1/\sqrt{2T_0})\sum_i (p_i)(n_i)^{-1}\Phi_0$ and $T^-\Phi_k^* = (1/\sqrt{2T_0})\sum_i (p_i)(n_i)^{-1}\Phi_k^*$, with $(p_i)(n_i)^{-1}$ representing a hole created in an occupied neutron orbital and a particle created in the corresponding proton orbital which together couple to zero angular momentum. The summations are over every occupied neutron orbital for which the corresponding proton orbital is empty.

Elastic scattering through the analog resonance occurs by absorption and emission of proton p_J in term I of Eq. (2). Decay of the analog state by emission of a charge-exchanged proton p_i from

term II,

$$\frac{\alpha\sqrt{2T_0}}{(2T_0+1)^{1/2}}(n_J \otimes T^- \Phi_0)$$

$$= \frac{\alpha}{(2T_0+1)^{1/2}}[n_J \otimes \sum_i (p_i)(n_i)^{-1}\Phi_0],$$

will leave the residual nucleus in a neutron particle-hole configuration. This will be referred to as mechanism II in the remainder of this text. Those excited states of the target nucleus Φ_k^* coupled to a neutron in the parent state will be populated by decay of protons p_j from term III. We will call this mechanism III. Neutron particle-hole configurations based on excited target states should result from the emission of charge-exchanged protons p_i in the decay of term IV in the same fashion as from term II.

In this present work, through the (d, p) and (p, p_0) experiments, we have measured the coefficients α in the expansion of the parent state. Through inelastic decay by mechanism III we can obtain information on the β_{jk} as well. In other experiments on even-even nuclei in the $N=82$ region,[24, 25] the first excited state (2_1^+) has been the only Φ_k^* of importance for low-lying resonances. That is,

$$\Psi_J \simeq \alpha(n_J \otimes \Phi_0) + \sum_j \beta_j (n_j \otimes \Phi_{2^+}), \quad (3)$$

with

$$\alpha^2 + \sum_j \beta_j \simeq 1 .$$

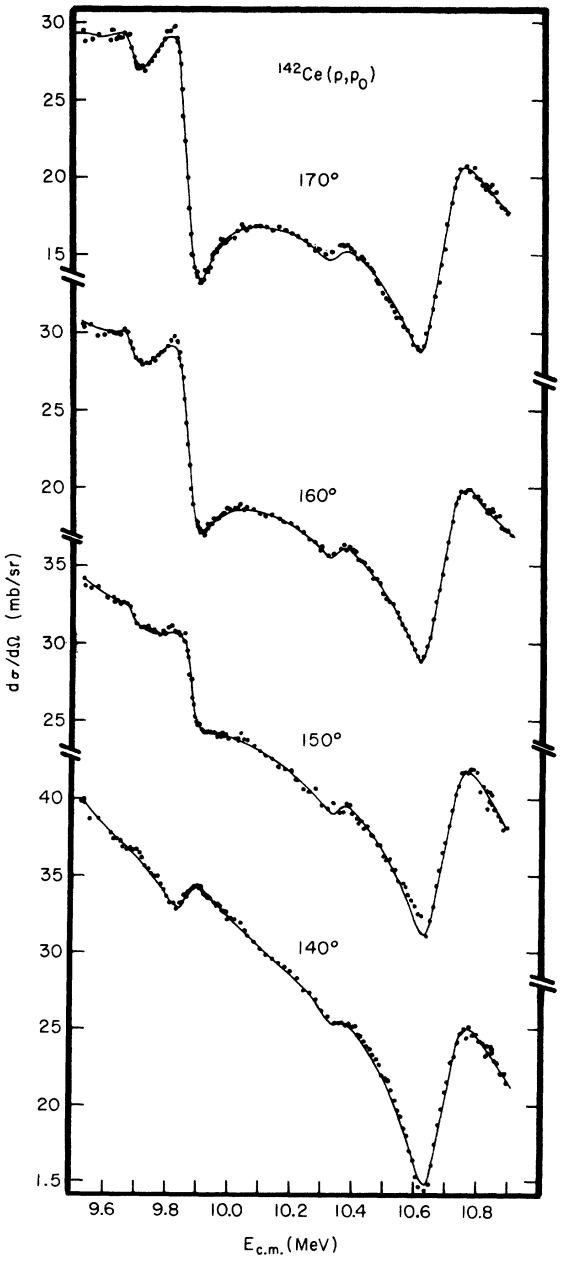

FIG. 8. Experimental cross sections for proton elastic scattering from ^{142}Ce and BRIGIT fits with parameters from Table V.

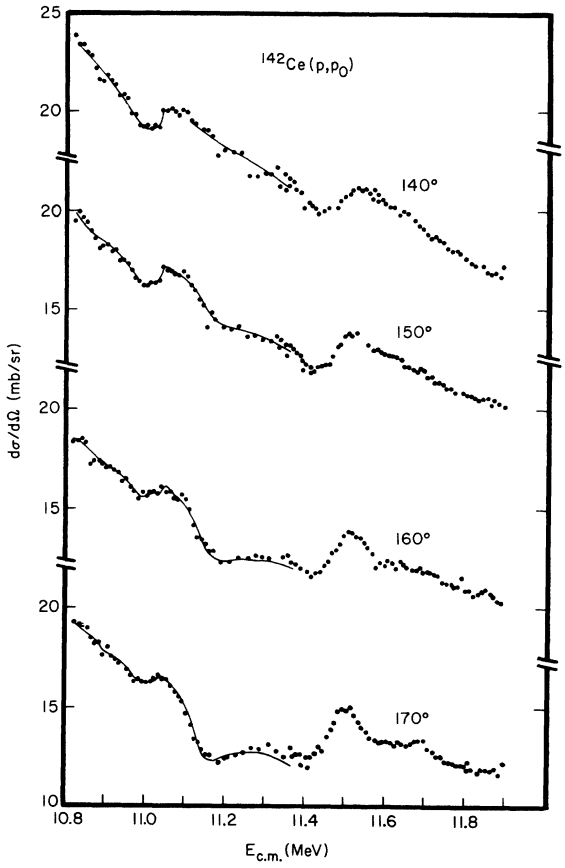

FIG. 9. Experimental cross sections for proton elastic scattering from ^{142}Ce and BRIGIT fits with parameters from Table V.

TABLE V. Results of ^{142}Ce(p, p) and comparison with ^{142}Ce(d, p). The quantities enclosed in parentheses are in some question.

^{142}Ce(p, p_0)							^{142}Ce(d, p)			
$E_{c.m.}$ (MeV)	$E_{c.m.}-9.844$ (MeV)	$\Gamma_{p_0}^{lJ}$ (keV)	Γ_T (keV)	l	J^π	S_{pp}	E_x (MeV)	l_n	J^π	S_{dp}
9.844	0.000	2.2±1	86.0±20	1	$\frac{3}{2}^-$	(0.07)	0.000	1	$\frac{3}{2}^-$	0.03
9.863	0.023	9.5±0.5	84.2±5	3	$\frac{7}{2}^-$	0.60	0.021	3	$\frac{7}{2}^-$	0.50
							0.668	5	$\frac{9}{2}^-$	0.26
10.654	0.810	19.0±1	110 ±10	1	$\frac{3}{2}^-$	0.45	0.815	1	$\frac{3}{2}^-$	0.50
10.712	0.868	10.5±1	80 ±10	1	$(\frac{1}{2}^-)$	0.30	0.869	1	$(\frac{1}{2}^-)$	0.32
11.002	1.158	2.5±1	59.5±20	1	$(\frac{1}{2}^-)$	(0.07)	1.162	1	$(\frac{1}{2}^-)$	0.07
11.035	1.191	1.4±1	34.3±20	1	$(\frac{1}{2}^-)$		1.178	1	$(\frac{1}{2}^-)$	0.04
11.045	1.201	2.3±1	101.9±30	3	$(\frac{5}{2}^-)$	(0.12)	1.195	3	$(\frac{5}{2}^-)$	0.11
							1.221	5	$\frac{9}{2}^-$	0.45
11.133	1.289	3.5±1	95.3±20	3	$(\frac{5}{2}^-)$	(0.17)	1.298	3	$(\frac{5}{2}^-)$	0.12

From the excitation curves the total resonant inelastic cross section σ_{pp_1} for the 2_1^+ state has been estimated. A first-order correction to the data was made by subtracting the off-resonance yield from the on-resonance cross section. The summation of the individual inelastic partial widths, $\sum_j \Gamma_{p_1}^j$, can be calculated from

$$\Gamma_{pp_1} = \frac{2\pi}{k^2}(2J+1)\frac{\Gamma_{p_0}^{lJ}}{\Gamma_T^{\,2}}\sum_j \Gamma_{p_1}^j . \qquad (4)$$

Three resonances are sufficiently well isolated so that a total-cross-section estimate can be made. These are the $\frac{7}{2}^-$, $\frac{3}{2}^-$, and $\frac{1}{2}^-$ resonances indicated in Table VII. While there are five odd-parity single-particle orbitals which can couple to the 2_1^+ state, the average spacing between them is ~500 keV. If we consider only the two lowest energy orbitals which can couple to the 2^+ state to give the J^π of the resonance, Eqs. (3) and (4) will permit the determination of their $\beta_j{}^2$.

In the case of closed-neutron-shell nuclei the states Φ_k^* of importance are either highly collective or involve only excited proton configurations, so that a level normally will be excited either by mechanism II or by mechanism III, but not by both. In the present case, the 2_1^+ first excited state will contain large components of ^{140}Ce ground state coupled to paired neutrons from the same orbital as the elastic channel. This will result in a significant component due to mechanism II in $\sum_j \Gamma_{p_1}^j$. The contribution from mechanism II, Γ_{II}^J, has been estimated from

$$\Gamma_{II}^J = \Gamma_{sp}^J \frac{2I+1}{J}\frac{S_{dp}}{U_J^{\,2}} V_J^{\,2} \left| \langle \Phi_{2^+} \,|\, \psi_0 \otimes (n_J)^2 \rangle \right|^2 ,$$

where J is the resonance spin, I is the final spin, $V_J^{\,2} = U_J^{\,2} - 1$ is the "fullness" of the subshell J in the ^{142}Ce ground state, Φ_{2^+} is the ^{142}Ce 2_1^+ wave function, and ψ_0 is the ^{140}Ce ground-state wave function.

This expression for Γ_{II}^J follows from the relation for a spectroscopic factor in proton inelastic decay of an analog resonance,[6] assuming mechanism II and a closed-neutron-shell target,

$$S_{pp_1} = \frac{\Gamma_{p_1}^j}{\Gamma_{sp}^J}\frac{2J+1}{2I+1} ,$$

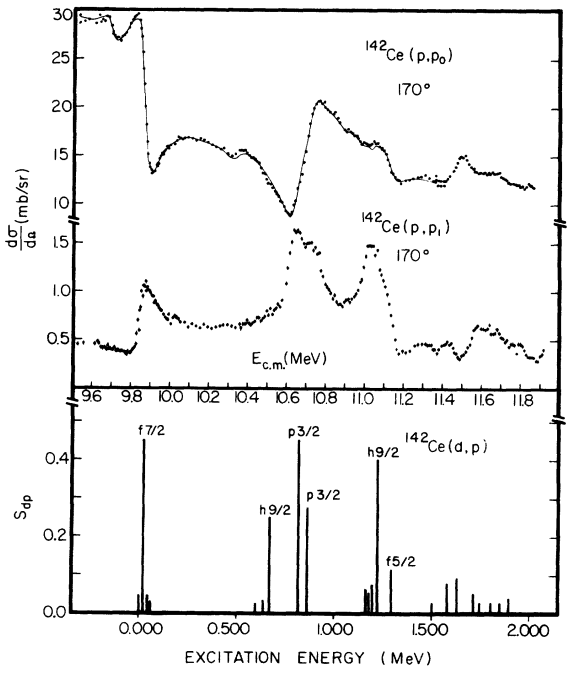

FIG. 10. Comparison of ^{142}Ce(p, p_1) 2_1^+ excitation function at 170° with elastic scattering excitation curve and the ^{142}Ce(d,p) spectrum.

TABLE VI. Inelastic partial widths and spectroscopic factors.

Res. No.	Excitation energy (MeV)	J^π	$\sigma_{p p_1}^{\text{total}}$ (mb)	$\sum_j \Gamma_{p_1}^j$ (keV)	Γ_{II}^J	$\sum_j \tilde{\Gamma}_{p_1}^j$ (keV)	$\tilde{\Gamma}_{p_1}^{f_{7/2}}$ (keV)	$\tilde{\Gamma}_{p_1}^{p_{3/2}}$ (keV)	$\tilde{\Gamma}_{p_1}^{h_{9/2}}$ (keV)	$\tilde{\Gamma}_{p_1}^{p_{1/2}}$ (keV)	$\tilde{\Gamma}_{p_1}^{f_{5/2}}$ (keV)	α^2	$\tilde{S}_{p_1}^{f_{7/2}}$	$\tilde{S}_{p_1}^{p_{3/2}}$	$\tilde{S}_{p_1}^{f_{5/2}}$
2	0.021	$\frac{7}{2}^-$	4.9	7.5	1.0	6.5	2.7	3.8	a	b	a	0.6	0.26	0.14	a
8	0.815	$\frac{3}{2}^-$	9.0	13.5	5.0	8.5	5.5	1.0	b	a	a	0.67	0.18	0.15	a
9	0.869	$(\frac{1}{2}^-)$	6.5	16.0	0.0	16.0	···	6.0	b	b	10.0	0.31	b	0.29	0.40

[a] Coupling allowed but omitted from calculation.
[b] Coupling not permitted by angular momentum considerations.

where j is the spin in the exit channel. Because $j=J$ in our case, the number of possible final states is restricted by the Pauli principle and

$$\frac{2J+1}{2I+1} \rightarrow \frac{J}{2I+1}.$$

We associate

$$S_{pp_1} = \frac{S_{dp}}{U_J^2} V_J^2 \left| \langle \Phi_{2^+} | \psi_0 \otimes (n_J)^2_{2^+} \rangle \right|^2 .$$

In our present procedure we have assumed

$$\left| \langle \Phi_{2^+} | \psi_0 \otimes (n_J)^2_{2^+} \rangle \right|^2 \simeq \left| \langle \Phi_0 | \psi_0 \otimes (n_J)^2_{0^+} \rangle \right|^2 = V_J^2 \frac{2J+1}{2}.$$

The quantity $V_J^2(2J+1)$ gives the total number of neutrons in subshell J contained in the ^{142}Ce ground state. Presumably there are two neutrons outside the closed shell and $V_J^2(2J+1)/2$ gives the fractional occupancy of the subshell J.

We may now obtain a summation of inelastic partial widths, $\sum_j \tilde{\Gamma}_{p_1}^j$, due only to mechanism III, the contribution from mechanism II having been subtracted. For a resonance of spin J

$$\sum_j \tilde{\Gamma}_{p_1}^j \simeq \sum_j \Gamma_{p_1}^j - \Gamma_{II}^J ,$$

$$\alpha^2 \simeq S_{dp}^J / U_J ,$$

and

$$\beta_j^2 = \tilde{\Gamma}_{p_1}^j / \Gamma_{sp}^j \equiv \tilde{S}_{p_1}(j)$$

with

$$\alpha^2 + \sum_j \beta_j^2 \simeq 1 .$$

Table VI shows the results of these considerations.

Our correction of $\sum_j \Gamma_{p_1}^j$ does not include some cross terms of unknown sign. We ignore contributions from mechanism IV. A more elaborate procedure is not justified because of lack of knowledge of Φ_{2^+}.

F. Coulomb Energies

From the resonance energies and (d, p) Q values, one can extract the Coulomb displacement energies ΔE_C using the relationship

$$\Delta E_C = E_p + Q_{dp} + 2.225 \text{ MeV},$$

where E_p is the c.m. proton energy at which the analog state in the nucleus $(N, Z+1)$ occurs, Q_{dp} is the (d, p) reaction Q value, and 2.225 MeV is the deuteron binding energy. The results for the main resonances are summarized in Table VII and compared with calculated values using the semiempirical relation[26]

$$\Delta E_C = b_1 \frac{\tilde{Z}}{A^{1/3}} + b_2 ,$$

where $\tilde{Z} = Z + \frac{1}{2}$ is the average charge of the isobaric analog pair, $b_1 = 1430 \pm 2.6$ keV, and $b_2 = -992 \pm 22.6$ keV. The observed value agrees with the calculated one within the experimental uncertainties.

TABLE VII. Coulomb displacement energies.

Target isotope	Analog pair	Q_{dp} (MeV)	E_p (MeV)	ΔE_C (MeV) Measured	ΔE_C (MeV) Calculated [a]
^{142}Ce	^{143}Ce-^{143}Pr	2.945	9.844	15.014	15.005 ± 0.040
		2.925	9.867	15.017	
		2.130	10.650	15.005	
		2.076	10.707	15.008	
		1.647	11.133	15.005	

[a] Reference 24.

IV. DISCUSSION AND INTERPRETATION

A. $^{142}Ce(d,p)$ and $^{142}Ce(p,p_0)$ Reactions

The level scheme obtained for ^{143}Ce is shown in Fig. 11 together with the $^{140}Ce(d,p)^{141}Ce$ results.[3,7] In the $^{142}Ce(d,p)$ experiment 55 states have been identified with l, the angular momentum transfer, assigned in 33 cases. The observed l values were all $l=1$, 3, or 5, in agreement with the shell-model predictions for the $N=82$ region. Apart from the $\frac{3}{2}^-$ ground state and the $\frac{7}{2}^-$ level[8] at 20 keV, all other states in ^{143}Ce were unknown.

The ground state shows an angular momentum transfer of $l=1$ consistent with the known $\frac{3}{2}^-$ spin. At an excitation energy of 20 keV a level with an $l=3$ angular distribution is identifiable as the $\frac{7}{2}^-$ state seen in the polarization experiment of Graw *et al.*[8] because of its large spectroscopic factor. There are two other states in the ground-state multiplet. The level at 40 keV is in the tail of the large 20-keV state, and no reliable angular distribution can be obtained; it is tentatively assigned as $l=1$ because of its large cross section at 20°, as compared with the $\frac{7}{2}^-$ level. The 58-keV state clearly shows an angular momentum transfer $l=3$.

In the region near 650 keV one might expect to find an $f_{7/2}$ neutron coupled to the ^{142}Ce 2^+ state at 641 keV. Four of the five levels of the resulting multiplet could be excited through admixtures

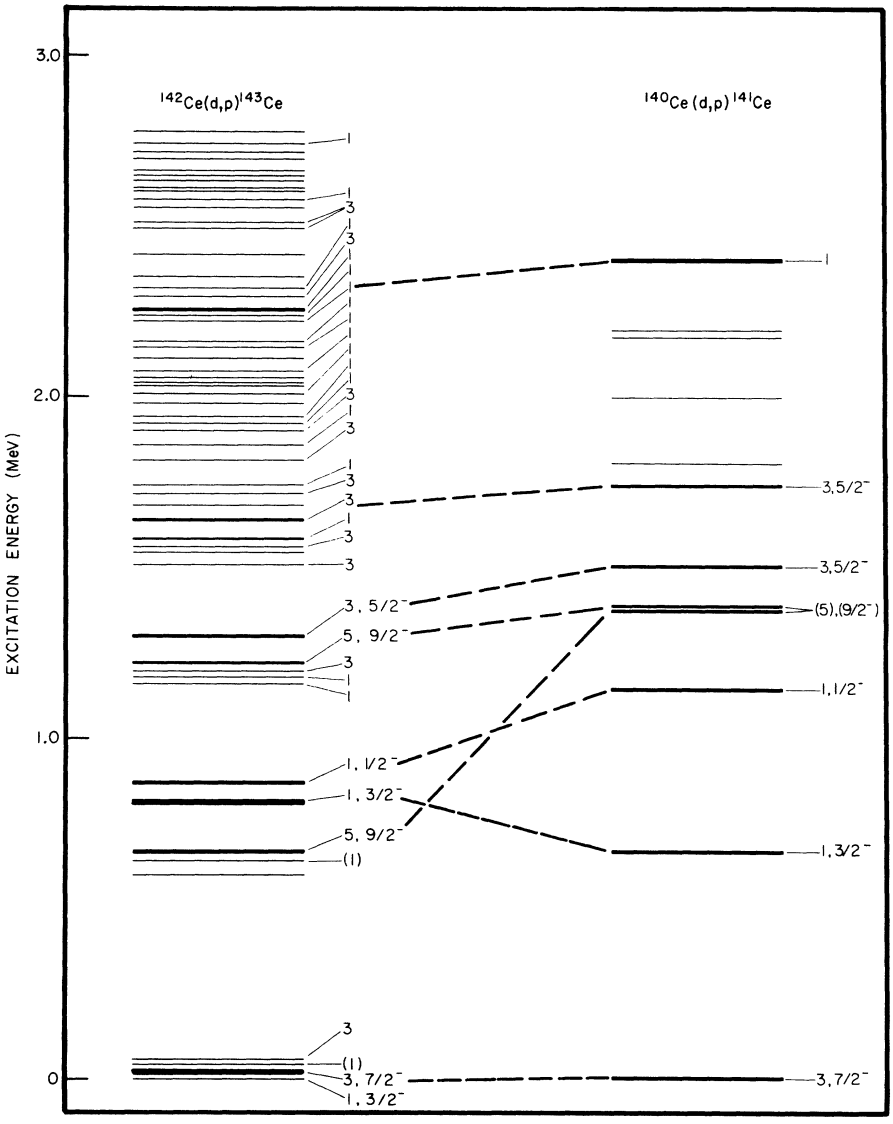

FIG. 11. Level schemes observed in $^{142}Ce(d,p)$ and $^{140}Ce(d,p)$ (Ref. 3). Those levels represented by broad lines are those with a large single-particle component.

of available neutron single-particle states. Three states are observed between 600 and 700 keV, all with small spectroscopic factors. Only the 668-keV level is sufficiently excited for a certain l assignment; $l=5$ with $S_{dp}=0.26$ is consistent only with $\frac{9}{2}^-$, one of the possible multiplet spins.

Two $l=1$ states occur between 800 and 900 keV. The level at 815 keV, $S_{dp}=0.5$, can be considered as the main component of the $3p_{3/2}$ single-particle level. A spectroscopic factor of $S_{dp}=0.50$ is consistent with the identification; for a spin of $\frac{1}{2}^-$ we would have $S_{dp}\simeq 0.9$, which is not realistic on the basis of comparison with ^{141}Ce. The 868-keV level might be identified as the strongest component of the $3p_{1/2}$ neutron level with $S_{dp}=0.32$, on the basis of comparison with ^{141}Ce.

Next, a group of five states is observed. The 1.162- and 1.178-MeV states have $l=1$ angular distributions. The $l=3$ levels at 1.195 and 1.298 MeV are probably $\frac{5}{2}^-$ from a comparison with the level scheme of ^{141}Ce and on the basis of available spectroscopic strength. The 1.221-MeV state with an $l=5$ angular distribution is the main $1h_{9/2}$ fragment with $S_{dp}=0.44$. No other J^π assignments are possible.

The excitation energies and spectroscopic factors from the proton elastic scattering analysis are in excellent agreement with the (d,p) results except for the ground state, which has $S_{pp}\simeq 2S_{dp}$. This could be the result of the ground-state analog resonance and the analog of the 40-keV level each being sufficiently broad so that their joint effect duplicates that of a single larger $l=1$ resonance. This tends to confirm our identification of the 40-keV level as having an $l=1$ angular distribution in the (d,p) experiment.

Considerably more fragmentation is seen in ^{142}Ce(d,p) than in ^{140}Ce(d,p), though the same number of major states are seen in the two experiments. The sum rules over the different values of l are still far from satisfied. Table VIII shows the values of $\sum(2J+1)S_{dp}$ for $l=1$, 3, and 5 with the fraction of available spectroscopic strength observed for each l, after correction for the occupancy of the $2f_{7/2}$ and $3p_{3/2}$ subshells obtained from the ^{142}Ce(d,t) experiment.

TABLE VIII. Summed spectroscopic factors for ^{142}Ce(d,p). S_l is the fraction of available spectroscopic strength observed:

$$S_l=\sum_i (2J+1)S^l_{dp}(i)/[\sum_J (2J+1)-\text{occupation}]\ .$$

J	l	$\sum(2J+1)S_{dp}$	$\sum(2J+1)$	Occupation	S_l
$2f_{7/2}$, $2f_{5/2}$	3	6.6	14	1.3	0.52
$3p_{3/2}$, $3p_{1/2}$	1	4.0	6	0.8	0.75
$1h_{9/2}$	5	6.4	10	···	0.64

A similar experiment was performed at about the same time as this present work by Seitz *et al.*,[27] using a large electromagnet in the scattering chamber to bend the deuteron elastic peak away from the detector. This should enable observations at more forward angles than was possible in this experiment and make the identification of the angular momenta transfer more certain.

B. ^{142}Ce(d,t) Reaction

The nucleus ^{142}Ce has two neutrons outside the closed $N=82$ shell. In the ^{142}Ce(d,t) reaction we expect to pick up neutrons from the occupied orbitals outside the closed shell and from the closed shell itself.

Four angular distributions were obtained. The ^{141}Ce ground state and first excited state were known to have spins of $\frac{7}{2}^-$ and $\frac{3}{2}^-$ with large $2f_{7/2}$ and $3p_{3/2}$ components. The state at 1.615 MeV with an $l=2$ angular momentum transfer should be $\frac{3}{2}^+$ on the basis of shell-model systematics. The 1.775-MeV level with $l=0$ must be $\frac{1}{2}^+$. Two other triton peaks were observed. The level at 1.065 MeV is the $\frac{1}{2}^-$ state known from the ^{140}Ce(d,p). The 2.140-MeV state is not seen at forward angles and is probably the major component of the $1h_{11/2}$ neutron hole level.

The spectroscopic factors are shown in Table IV. The ground state of ^{142}Ce shows occupancy of only the $2f_{7/2}$ and $3p_{3/2}$ subshells outside the closed shell, in general agreement with the description given by Fulmer, McCarthy, and Cohen. The spectroscopic factors for the $\frac{3}{2}^+$ and $\frac{1}{2}^+$ states are significantly lower than the $2d_{3/2}$ and $3s_{1/2}$ spectroscopic factors for the reactions ^{140}Ce$(d,t)^{139}$Ce.

C. ^{142}Ce(p,p_1) Reaction

As was discussed in Sec. III, it was possible to account for essentially all of the decay of the analog resonances in the $N=82$ nuclei plus proton systems by including coupling to the 2^+_1 core state. In the case of ^{143}Ce, one should expect a still larger coupling to the 2^+_1 core state in ^{142}Ce, because of the lower excitation energy of this state (641 keV) compared with the energy of the corresponding state in ^{140}Ce (1.596 MeV).

The structure of the 2^+_1 excitation function shows coupling not only to those states with large single-particle components but also to the fragments observed around the $f_{7/2}$ state and those in the region of the principal $h_{9/2}$ component. No significant structure appears in the 2^+_1 excitation function in the energy range corresponding to excitation en-

ergies 1.3 to 2.0 MeV.

The contributions to the parent states of 2_1^+ and the other excitation modes of the core can, in principle, be derived from the inelastic decay properties of the analog resonances. In this present work, through a number of assumptions, we have attempted to determine the complete wave function for three states of ^{143}Ce in terms of ^{142}Ce ground state and 2_1^+ state coupled to the two lowest-energy neutron single-particle orbitals which may couple to the proper spin with the 2_1^+. The results were

$$\Psi_{7/2^-} \simeq \pm\sqrt{0.6}(f_{7/2} \otimes 0^+) \pm \sqrt{0.26}(f_{7/2} \otimes 2_1^+) \pm \sqrt{0.14}(p_{3/2} \otimes 2_1^+)$$

for the 20-keV level,

$$\Psi_{3/2^-} \simeq \pm\sqrt{0.67}\,(p_{3/2} \otimes 0^+) \pm \sqrt{0.18}\,(f_{7/2} \otimes 2_1^+) \pm \sqrt{0.15}\,(p_{3/2} \otimes 2_1^+)$$

for the 815-keV level, and

$$\Psi_{1/2^-} \simeq \pm\sqrt{0.31}\,(p_{1/2} \otimes 0^+) \pm \sqrt{0.29}\,(p_{3/2} \otimes 2_1^+) \pm \sqrt{0.40}\,(f_{5/2} \otimes 2_1^+)$$

for the 865-keV level.

While these results should be considered as very approximate, they are in basic agreement with those of Hiddleston and Riley[24] and Clement *et al.*[25] As might be expected, the 4^+ level at 1.219 MeV is by far the most strongly excited level apart from the 2_1^+. The 4^+ level, while resonating strongly on the $f_{7/2}$ resonance because of its large $[(n_{f_{7/2}})^2 \otimes {}^{140}\text{Ce}$ ground-state$]$ component had only about 4% of the 2^+ cross section on the $\frac{3}{2}^-$ and $\frac{1}{2}^-$ resonances, indicating that considering only the 2^+ is justified to first order. Failure to include coupling of the $h_{9/2}$ neutron to the 2^+ state for the $\frac{7}{2}^-$ resonance could be a serious omission, as could be the failure to consider interference between resonant and nonresonant processes.

ACKNOWLEDGMENTS

We are deeply grateful to Professor Pierre Depommier for his support and encouragement of this work. Roger Martin provided considerable assistance in the taking of the data. We acknowledge helpful conversations with Professor Claude Mahaux and Dr. Roch Mercier.

---

†Work supported by the National Research Council of Canada.

*On leave from Institut de Physique Nucléaire, Orsay, France.

[1]A. Chaumeaux, G. Bruge, H. Faraggi, and J. Picard, Nucl. Phys. A164, 176 (1971).

[2]R. K. Jolly and E. Kashy, Phys. Rev. C 4, 887 (1971).

[3]C. A. Wiedner, A. Heusler, J. Solf, and J. P. Wurm, Nucl. Phys. A103, 443 (1967).

[4]G. C. Morrison, N. Williams, J. A. Nolen, Jr., and D. Von Ehrenstein, Phys. Rev. Letters 19, 592 (1967).

[5]P. A. Moore, P. J. Riley, C. M. Jones, M. D. Mancusi, and J. L. Foster, Jr., Phys. Rev. Letters 22, 356 (1969).

[6]G. C. Morrison, in *Nuclear Isospin*, edited by J. D. Anderson, S. D. Bloom, J. Cerny, and W. W. True (Academic, New York, 1969).

[7]R. H. Fulmer, A. L. McCarthy, and B. L. Cohen, Phys. Rev. 128, 1302 (1962).

[8]G. Graw, G. Glausnitzer, R. Fleischmann, and K. Wienhard, Phys. Letters 28B, 583 (1969).

[9]C. Maples, G. W. Goth, and J. Cerny, Nucl. Data A2, 429 (1966).

[10]S. Liran and N. Zeldes, Nucl. Phys. A136, 217 (1969).

[11]R. Raynal, Internal Report MAGALI, Centre d'Etudes Nucléaires, Saclay, France (unpublished).

[12]F. G. Perey, Phys. Rev. 132, 755 (1963).

[13]C. M. Perey and F. G. Perey, Phys. Rev. 132, 755 (1963).

[14]F. D. Becchetti, Jr., and G. W. Greenlees, in *Polarization Phenomena in Nuclear Reactions*, edited by H. H. Barschall and W. Haeberli (University of Wisconsin, Madison, 1970).

[15]P. D. Kunz, University of Colorado, Program DWUCK (unpublished).

[16]G. R. Satchler, Nucl. Phys. 55, 1 (1964).

[17]R. H. Bassel, Phys. Rev. 149, 156 (1966).

[18]W. J. Thompson, J. L. Adams, and D. Robson, Phys. Rev. 975 (1968).

[19]H. Feshbach, in *Nuclear Spectroscopy*, edited by F. Ajzenberg-Selove (Academic, New York, 1960), Pt. B, p. 625.

[20]C. F. Moore and L. Parish, University of Texas, Center for Nuclear Studies, Technical Report No. 2, 1967 (unpublished).

[21]S. A. A. Zaidi, J. L. Parish, J. G. Kulleck, and C. F. Moore, Phys. Rev. 165, 1312 (1968).

[22]N. Williams, G. C. Morrison, J. A. Nolen, Jr., Phys. Rev. C 2, 1539 (1970).

[23]J. P. Wurm, A. Heusler, and P. von Brentano, Nucl. Phys. A128, 433 (1969).

[24]H. R. Hiddleston and P. J. Riley, Phys. Letters 32B, 425 (1970).

[25]H. Clement, G. Graw, W. Kretschmer, and P. Schulzs-Dobold, Phys. Rev. Letters 27, 526 (1971).

[26]J. Jaenecke, in *Isospin in Nuclear Physics*, edited by D. H. Wilkinson (North-Holland, Amsterdam, 1969).

[27]H. Seitz, S. A. A. Zaidi, R. Bigler, and J. Horton, Bull. Am. Phys. Soc. 16, 538 (1971).